

First-principles calculations of defect-induced lattice relaxation in ionic systems

Koblar Jackson, Mark R. Pederson, and Barry M. Klein

*Complex Systems Theory Branch, Condensed Matter and Radiation Sciences Division,
Naval Research Laboratory, Washington, D.C. 20375-5000*

(Received 27 June 1990; revised manuscript received 17 September 1990)

Local-density-approximation methods are used to investigate defect-induced lattice relaxation in $\text{LiCl}:\text{Cu}^+$ and for the F center in MgO . Calculations are carried out on large finite clusters of atoms using a linear combination of atomic orbitals (LCAO)-type basis set, and defect-related properties are deduced from a comparison of results for related pure and defect clusters. The outer atomic shells of these clusters are allowed to relax, to respond to effects of truncating the clusters at finite sizes. We show that, with this relaxation, the calculated electronic and structural properties of the pure clusters are good approximations to the corresponding bulk properties. Using the finite-cluster procedure, we find essentially no relaxation of the defect near-neighbor ions in $\text{LiCl}:\text{Cu}^+$, but an inward relaxation of 1.3% of the near-neighbor ions around the F center in MgO .

I. INTRODUCTION

An accurate description of the properties of point defects in solids should include the relaxation of bulk crystal atoms around the defect, since the formation energy of the defect and the positions of defect-related levels with respect to host crystal bands can both be strongly affected by relaxation. However, experimental measurements of defect-induced lattice relaxation are difficult to make, so that precise data are largely lacking. Calculating the relaxation is also difficult. Most methods for treating the defect problem can allow for relaxation of host atoms in principle, but in practice, defect-induced lattice relaxation is often ignored. Many methods are formulated with the pure undistorted host crystal as a reference for the defect system, and allowing relaxation of the atoms near the defect makes the calculations extremely complicated and costly.

In this paper we discuss an approach to the defect-induced lattice relaxation problem based on free, finite atomic clusters. By effectively treating only the region of the solid in the immediate vicinity of the defect, the finite-cluster approach can be used to investigate defect-induced relaxation effects directly. Conceptually, our approach is based on the fact that the local atomic environment in the interior of a sufficiently large cluster is indistinguishable from that of the bulk, so that cluster estimates of bulk properties extracted from the central region of a cluster can be expected to converge to the bulk values in the large cluster limit. It is not known how large a cluster must be treated in order to ensure full convergence to bulk properties, and we do not set out in this work to address this question. Instead we apply the cluster formalism in a pragmatic way to determine the feasibility of the approach for estimating bulk properties, particularly those relating to point defects, using moderately sized clusters.

The equilibrium atomic positions in the finite cluster are somewhat shifted from the corresponding equilibrium

positions in the bulk solid due to stresses introduced by truncating the cluster at a finite size. Allowing the atomic shells in the cluster to relax from the ideal bulk lattice positions counteracts these truncation effects and provides a more physically meaningful boundary for the clusters. Accordingly, we expect that estimates of bulk properties taken from relaxed clusters converge to the bulk values faster than those taken from unrelaxed clusters. This point can be made more general. Allowing the cluster to relax to its full variational ground state gives the cluster its greatest opportunity to respond to truncation effects, and we expect that by optimizing the cluster energies with respect to all structural and electronic degrees of freedom, we will obtain the fastest and smoothest convergence to the bulk values.

The defect-related properties reported here are obtained from a comparison of calculations of pure clusters and the corresponding "defect" clusters, containing a single point defect. We have used this approach to investigate lattice relaxation around the Cu^+ substitutional impurity in LiCl , and the F center in MgO . These represent prototypical defect systems, and have been studied in the past using various methods.¹⁻⁴

The paper is organized as follows: in the next section we provide a brief overview of our computational approach, and discuss in more detail the use of finite clusters to obtain estimates of bulk properties. In Sec. III we present our results, for $\text{LiCl}:\text{Cu}^+$ and for the MgO F center. We include in this section a comparison with results obtained in previous studies. In the final section we summarize, offering our conclusions regarding this work and suggesting possible future directions.

II. THEORY

Our calculations are based on the Hohenberg-Kohn-Sham local-density approximation⁵ (LDA), which we use to study the structural and electronic properties of finite atomic clusters. In the LDA, the ground-state energy (in

Hartree atomic units) of an N electron system is written as a function of the nuclear coordinates, \mathbf{R}_ν , and a functional of the electronic charge density ρ :

$$E = \frac{1}{2} \sum'_{\nu,\mu} \frac{Z_\nu Z_\mu}{|\mathbf{R}_\nu - \mathbf{R}_\mu|} + 2 \sum_i \langle \psi_i | (-\frac{1}{2} \nabla^2 + V_{\text{ext}}) | \psi_i \rangle + \frac{1}{2} \int d\mathbf{r} \int d\mathbf{r}' \frac{\rho(\mathbf{r})\rho(\mathbf{r}')}{|\mathbf{r} - \mathbf{r}'|} + \int d\mathbf{r} \rho(\mathbf{r}) \epsilon_{\text{xc}}[\rho], \quad (1)$$

where

$$V_{\text{ext}} = - \sum_\nu \frac{Z_\nu}{|\mathbf{r} - \mathbf{R}_\nu|}, \quad (2)$$

and

$$\rho(\mathbf{r}) = 2 \sum_{i=1}^N |\psi_i(\mathbf{r})|^2. \quad (3)$$

Here \mathbf{R}_ν is the position of and Z_ν the charge of the ν th nucleus. The density is determined from the one-electron wave functions, the ψ_i 's. Schrödinger-like equations for the ψ_i 's are derived from Eq. (1) variationally, yielding

$$[-\nabla^2/2 + V_{\text{eff}}(\mathbf{r})] \psi_i(\mathbf{r}) = \lambda_i \psi_i(\mathbf{r}), \quad (4)$$

where

$$V_{\text{eff}} = V_{\text{ext}} + \int d\mathbf{r}' \frac{\rho(\mathbf{r}')}{|\mathbf{r} - \mathbf{r}'|} + \frac{\partial}{\partial \rho} (\rho \epsilon_{\text{xc}}[\rho]). \quad (5)$$

We solve Eq. (4) using a linear combination of atomic orbitals (LCAO) approach with Gaussian-based basis orbitals. We have described the details of our procedure elsewhere,⁶ so here we outline only the key aspects of our approach. First, the use of a Gaussian-orbital basis set allows an essentially exact representation of the LDA effective potential V_{eff} . With the wave functions expressed in terms of Gaussian-type functions, the electronic Coulomb potential can be evaluated analytically (in terms of the error function) from the charge density. In practice, we break the density up into short- and long-range pieces, and evaluate the Coulomb potential separately for the two parts. The potential due to the short-range part can be accurately and efficiently evaluated via a decomposition of the density into moments,⁷ while the potential for the long-range part of the density is obtained analytically. The remaining parts of V_{eff} , the nuclear and exchange-correlation potentials, may be readily tabulated exactly on a mesh of points. We evaluate the matrix element integrals required for solving Eq. (4) numerically, using a variationally determined integration mesh. The accuracy of these integrals may be systematically controlled, so that the matrix elements for the electronic structure problem can be evaluated to arbitrary accuracy.⁶

In the LDA, structural properties are determined by calculating the LDA total energy as a function of nuclear coordinates, the lowest-energy configuration being the LDA ground state. For the work described here static geometry optimizations were performed, i.e., the minimum-energy structures were found by systematically varying the nuclear coordinates in a sequence of calculations. The LDA eigenvalues are used to study the cluster

electronic structure. In the ionically bonded clusters studied in this work, the cluster eigenvalues fall in bands corresponding to the bulk crystal band structure. With increasing cluster size, the bands are populated by increasing numbers of discrete cluster energy levels, broadening and coalescing into the bulk energy bands in the large cluster limit. As for a bulk system, the energy band gap for a cluster is defined as the energy difference between the highest occupied valence state and the lowest unoccupied conduction state.

Since, in the limit of large clusters, the atomic and electronic environment of the cluster interior coincides exactly with that of the bulk system, point defects in large clusters can be expected to manifest bulklike defect properties. We identify defect-related properties by comparing the results of parallel calculations carried out on a pure cluster and the corresponding cluster with a central point defect. In this work, the clusters are formed by placing atoms on ideal lattice sites around a central atom, truncating the cluster at a specified number of shells of atoms. The atomic shells are then allowed to relax to minimize the cluster energy and to thereby provide a physically reasonable boundary for the cluster. As we shall show in the next section, allowing this relaxation is a key step in obtaining bulklike properties from the cluster.

III. RESULTS

A. LiCl:Cu⁺

Cu⁺ is known to be an on-site impurity in the LiCl lattice,⁸ substituting for one of the Li⁺ ions. Because of the difference in the ionic radii, 0.78 Å versus 0.96 Å for Li and Cu, respectively, one might expect significant outward relaxation of the near-neighbor Cl ions around the impurity in LiCl:Cu⁺. However, Harrison and Lin⁹ have noted that the atomic spacing in zinc-blende-structure CuCl, 2.35 Å, is significantly smaller than that in rock-salt LiCl, 2.57 Å. They use a scaling argument to estimate an atomic spacing of 2.52 Å for a hypothetical rock-salt CuCl for comparison with LiCl, and suggest that relaxation in LiCl:Cu⁺ should be much smaller than the difference in ionic radii, and possibly inward.

To study this system, we performed calculations on 27-atom clusters, corresponding to a central atom and the (100), (110), and (111) near-neighbor shells in the bulk-crystal rock-salt structure. The unrelaxed cluster geometry is shown in Fig. 1. With a cation atom at the center, the cluster contains 13 cation atoms and 14 anion atoms. Because of the mismatch in the number of cations and anions, the electronic structure of the neutral cluster corresponds to that of a bulk insulator with a hole in the valence band. The neutral cluster thus does not correspond to a collection of full-closed-shell ions, as is the case in the bulk solid. Furthermore, since the Cu⁺ 3*d* states fall in the host-crystal band gap, the neutral defect cluster would have an unoccupied impurity *d* state, and would correspond to a Cu²⁺ defect system. To provide a better analogue of the respective bulk systems, we add an extra electron to both the pure and defect clusters, giving

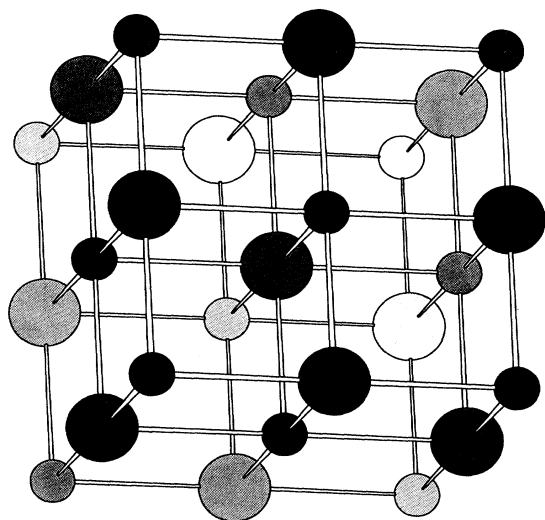


FIG. 1. The unrelaxed 27-atom cluster used in this work. The different atom types are represented by different-sized spheres; depth is indicated by shading, with the darkest atoms closest to the reader.

each a net charge of -1 .

The question of the cluster charge state can be approached from a more fundamental point of view, by requiring that the total energy of the cluster be minimized with respect to the number of electrons in the cluster. As mentioned in the Introduction, we expect that allowing a cluster to relax to its full variational ground state allows the system to respond as much as possible to effects of truncating the cluster at finite size, and properties extracted from cluster ground states are expected to converge most smoothly to bulk properties. In accordance with Janak's theorem,¹⁰ the energy of the negatively charged system, corresponding to a filled valence band, is lower than that of the cluster with a valence-band (VB) hole (the VB eigenvalues are negative). We therefore choose to study negatively charged clusters for the $\text{LiCl}:\text{Cu}^+$ problem because they better represent the true ground states of the pure and defect systems.

To investigate the relaxation of the near-neighbor Cl ions around the impurity, we studied first the pure cluster, and then the corresponding cluster with Cu substituted for the central Li atom. We allowed these clusters to relax using the following procedure. First, while constraining the clusters to maintain the perfect rock-salt structure [atoms at $(0,0,0)$, $(a,0,0)$, $(a,a,0)$, and (a,a,a) , and all the sites equivalent to these by octahedral symmetry], we minimized the cluster total energy as a function of the near-neighbor spacing a . Figure 2(a) is a plot of the total energy versus a for this breathing-mode relaxation for the 27-atom LiCl cluster. The curve in Fig. 2(a) has a minimum at $a = 4.57$ a.u., a 6% contraction over the bulk near-neighbor separation of 4.86 a.u. This contraction can be thought of as a response of the atoms in the cluster to the formation of the cluster surface.

From the energy minimum of the breathing-mode re-

laxation, we allow the first near-neighbor ions to further relax while holding the remaining ions fixed. Further relaxation of the second and third atomic shells does not significantly change the position of the first shell after this second relaxation step. The spacing between the central atom and first near-neighbor shell obtained at the minimum of this second relaxation step is taken as the cluster estimate of the bulk near-neighbor separation. Figure 2(b) depicts the second relaxation step for the pure LiCl cluster. The first near-neighbor shell is seen in Fig. 2(b) to relax outward to 4.91 a.u., in close agreement with the experimental bulk near-neighbor spacing of 4.86 a.u.

To investigate the importance of the initial breathing-mode relaxation, we allowed the first near-neighbor shell to relax from the unrelaxed cluster starting point, i.e., without first performing the breathing relaxation. The results are depicted by the squares in Fig. 2(b). Without the preliminary breathing relaxation, the first-neighbor relaxation yields a minimum-energy near-neighbor spacing of 4.97 a.u., a much worse estimate of the bulk near-neighbor spacing than that obtained using both relaxation steps.

To obtain a cluster estimate for the lattice relaxation around Cu^+ we repeat the second relaxation step for the defect cluster, starting from the energy minimum of the breathing-mode relaxation. The energy versus near-neighbor relaxation curve for the $\text{LiCl}:\text{Cu}^+$ cluster is also shown in Fig. 2(b). This curve has a minimum at 4.92 a.u., essentially the same value as for the pure cluster. The cluster calculations thus predict minimal lattice relaxation around the impurity ion. This result is at odds with a simple comparison of Cu^+ and Li^+ free ion radii, but is in qualitative agreement with the argument of Harrison and Lin.⁹

The $\text{LiCl}:\text{Cu}^+$ electronic structure gives some insight into why the simple comparison of free ion radii may not yield a good approximation for the defect-induced relaxation in $\text{LiCl}:\text{Cu}^+$. While the occupied states in the LiCl cluster are either anion-derived or cation-derived, as in bulk LiCl (e.g., the Cl $3p$ valence band), analyzing the LCAO eigenvectors for the $\text{LiCl}:\text{Cu}^+$ ground state shows the impurity gap states to be a linear combination of Cu $3d$ orbitals and first near-neighbor Cl $3p$ orbitals. This mixing of impurity (cation) and host (anion) orbitals arises due to overlap of the free ion Cu^+ and Cl^- orbitals in the fixed basis set, confirming that the simple picture of a free Cu^+ ion embedded in the LiCl crystal is only a qualitative representation of the true ground state. The host and impurity orbitals mix to form bonding and antibonding combinations of states, all of which are occupied. In addition, there is significant admixture of the Cu $4s$ orbital into the occupied valence states of A_{1g} symmetry. (A Mulliken population analysis¹¹ of the eigenvectors assigns about 0.2 units of electron charge to the Cu^+ site due to this mixing.) In this case, only the bonding combination of the Cu $4s$ and Cl $3p$ states is occupied, enhancing the bonding between the Cu atom and its near neighbors, resulting in a shorter near-neighbor distance than implied by the sum of free ion radii.

It is possible that the details of this host-impurity bonding would change somewhat as a function of cluster

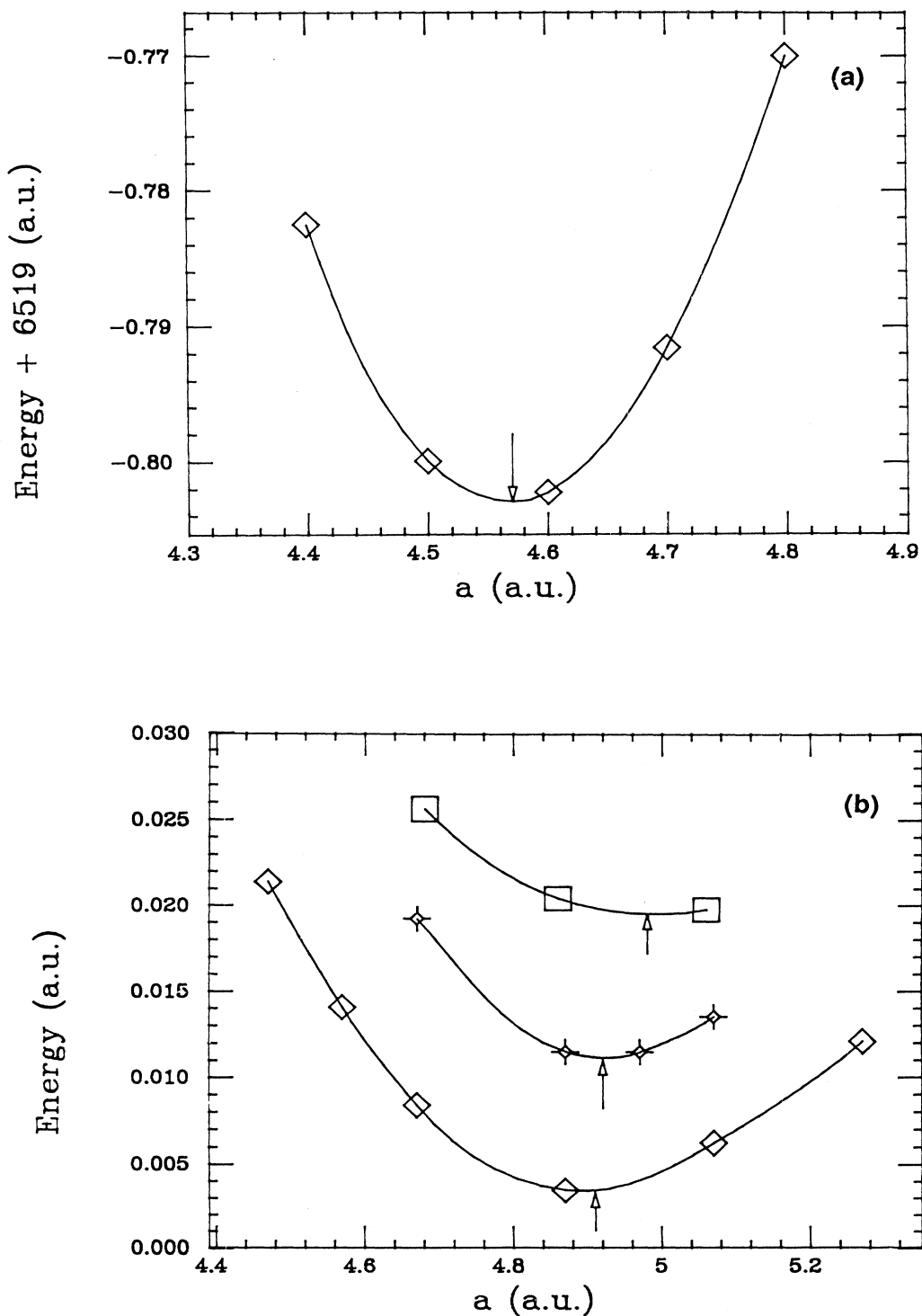


FIG. 2. (a) Total energy vs near-neighbor separation for the pure LiCl cluster breathing-mode relaxation. The minimum is at 4.57 a.u. Energies are quoted in Hartree atomic units. (b) Total energy vs the first near-neighbor distance for the LiCl and LiCl:Cu⁺ clusters. The diamonds correspond to the independent relaxation of the first-neighbor atomic shell in the pure LiCl cluster from the breathing-mode minimum of 4.57 a.u. The squares represent first-neighbor relaxation in the LiCl cluster from the unrelaxed atomic positions (all near-neighbor distances set equal to the bulk value of 4.86 a.u.). The crosses correspond to first shell relaxation in the LiCl:Cu⁺ cluster from the breathing-mode minimum (all near-neighbor distances equal to 4.57 a.u.). The energy scales for the three curves are shifted for presentation. The minima of the three curves are marked by arrows in the figure and fall at 4.91, 4.97, and 4.92 a.u., respectively. Energies are quoted in Hartree atomic units.

size, due, for example, to changes in the long-range Madelung potential at the defect and first-neighbor Cl sites. We expect the bonding to be dominated by local effects, however, such as charge transfer between the defect and its near neighbors. Such effects should be well described in the clusters studied here, and we therefore expect the cluster estimate of the lattice relaxation given here to be reliable. It would be interesting to study the host-impurity bonding as a function of cluster size, but such a study is outside the scope of the present work.

It is reasonable to consider the effect of treating negatively charged clusters on the relaxation result since the additional charge may also affect the bonding in the clusters. Because the neutral defect cluster corresponds to a Cu^{2+} impurity, as mentioned above, it does not make sense to repeat the above calculations using neutral clusters. For reference, however, we repeated the pure-cluster calculations using a neutral cluster, to gauge the effect of the extra electron on the results. Using the two-step relaxation process described above, we find a result of 4.88 a.u. for the near-neighbor distance. This is quite similar to the 4.91 a.u. result found above for the negatively charged cluster, so that the extra electron has only a small effect on the pure-cluster binding. It is reasonable to expect that the extra electron would have a similarly small effect on the defect cluster as well, and thus should not greatly influence the defect-induced lattice relaxation result.

B. The MgO *F* center

The neutral *F* center in MgO consists of two electrons bound to an oxygen vacancy. Like LiCl, MgO also has the rock-salt structure, and to study this system we again used the 27-atom cubic cluster shown in Fig. 1. Because of our interest in the *F* center, we construct the cluster with an anion atom at the origin, giving a total of 14 Mg atoms and 13 O atoms in the pure cluster. Because of the unpaired Mg atom, the ground-state electronic structure for the neutral cluster has two extra electrons outside a filled oxygen *2p* valence band. These electrons occupy surface states which fall in what corresponds to the pure-crystal band gap. Although the *F*-center states in the defect cluster also fall in the host band gap, these states are well separated from the surface states, lying about 2.5 eV lower in energy than the surface states, and there is no ambiguity in distinguishing them. In these clusters, adding or removing electrons causes the cluster energy to increase, so we choose to study neutral clusters in this case, in contrast to the LiCl case just discussed.

To investigate lattice relaxation around the *F* center, we followed a procedure similar to that discussed above for $\text{LiCl}:\text{Cu}^+$, treating first the pure and then the defect cluster. Because relaxation of the second-neighbor shell of atoms has been reported to be important in determining the magnitude of the first-neighbor shell relaxation, we relax each near-neighbor shell of atoms around the central atom independently. In this way we can gauge the effects of relaxation beyond the two-step process described above for LiCl, and consistently allow for second-neighbor relaxation in the *F*-center cluster. The

minimum-energy configuration for the pure cluster is found to be $a = 3.88$ a.u., $b = 3.80$ a.u., and $c = 3.70$ a.u., where the first atomic shell is at $a(1,0,0)$, the second at $b(1,1,0)$, and the third at $c(1,1,1)$. The measured atomic spacing in bulk MgO is 3.98 a.u., so that the cluster estimate of 3.88 a.u. underestimates the bulk value by 2.5%.

Figure 3(a) is a contour plot of the total energy of the

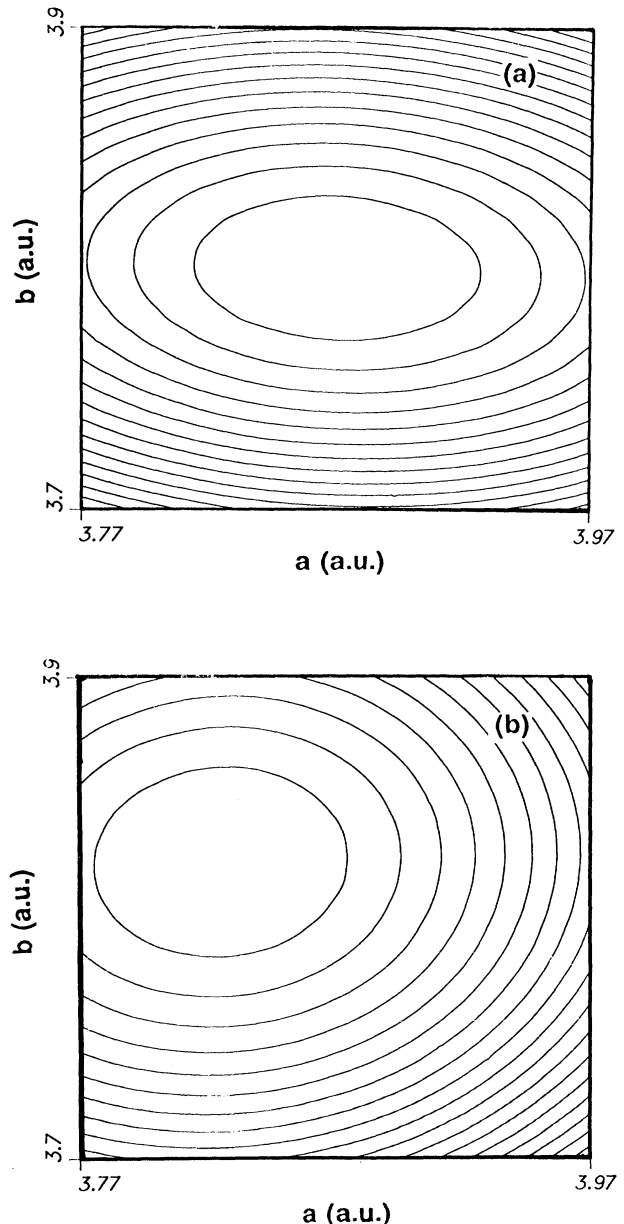


FIG. 3. Contour plots of the energy surface in the region of the minimum-energy configurations for the pure MgO (a) and *F*-center clusters (b). The energy is plotted vs a and b , the shell parameters for the first and second atomic shells [atoms at $a(1,0,0)$ and $b(1,1,0)$]. The third shell parameter is fixed at its value at the energy minimum for the MgO cluster, 3.70 a.u. The contours were generated from quadratic fits of the calculated total-energy data.

TABLE I. The atomic shell parameters for the minimum-energy MgO clusters. The atoms are on the atomic shells given by $a(1,0,0)$, $b(1,1,0)$, and $c(1,1,1)$. The central cluster site defines the origin, $(0,0,0)$. For the F center cluster, the third-neighbor shell is held fixed at 3.70 a.u. The shell parameters a , b , and c are given in a.u.

	Pure cluster	F -center cluster
a	3.88	3.83
b	3.80	3.83
c	3.70	3.70

pure MgO cluster versus a and b . To generate the plot, the third shell parameter was held fixed at its minimum-energy value, 3.70 a.u. The contours were generated from a quadratic fit to 27 calculated total-energy points near the minimum. The asymmetry of the contours in Fig. 3 indicates the greater energy cost of moving the (110) shell of atoms compared to the (100) shell, due to the greater number of atoms in the (110) shell (12 versus 6).

For the F -center cluster, we fixed the position of the outermost shell at $c=3.70$ and relaxed the inner two shells around the central O vacancy. Figure 3(b) is the analogous contour plot for the energy in the F -center cluster, based on 11 total-energy calculations to determine the energy as a function of the two parameters a and b . The minimum-energy coordinates for the F -center cluster were found to be $a=3.83$ and $b=3.83$ a.u. In comparison with the pure cluster, the first near-neighbor shell relaxed inward around the F center by 1.3%, while the second-neighbor shell relaxes outward by about 0.7%. From the symmetry of the contours in Fig. 3(b), it can be seen that the inward relaxation of the first neighbors stiffens that relaxation mode relative to the second-neighbor relaxation, compared to the pure cluster. The minimum-energy coordinates for the pure and F -center clusters are summarized in Table I.

C. Cluster estimates of pure-crystal properties

It is interesting to compare the estimates of MgO and LiCl properties determined from the pure-cluster calculations with the corresponding bulk values, as it gives an indication of the degree to which the cluster based results reproduce bulk properties and serves as a check on the defect relaxation results. In Table II we present a comparison of cluster and bulk properties for MgO, including both measured and calculated LDA values for the bulk systems.¹²⁻¹⁴ The cluster value for the MgO band gap is taken from the minimum-energy cluster as the energy difference between the highest occupied valence state, and the lowest unoccupied conductionlike state. As discussed earlier, the $\text{Mg}_{14}\text{O}_{13}$ cluster has a set of surface states in the band gap, but these are readily identified and are not considered in determining the gap. The position of the F -center level is taken from the minimum-energy defect cluster, and is defined as the energy difference between the highest valence state and the F -center state. The cluster near-neighbor distance, taken from the minimum-energy pure cluster, is defined as the distance

TABLE II. Cluster estimates of bulk properties versus the corresponding values taken from experiment and bulk LDA calculations. The procedures for obtaining the cluster estimates are described in the text.

	MgO		
	Cluster	Bulk LDA	Expt.
Band gap (eV)	4.80	4.65 ^a	7.80
Atomic spacing (a.u.)	3.88	3.94 ^b	3.98
Bulk modulus (Mbar)	1.86	1.72 ^b	1.56
F -center level (eV)	3.51	2.55 ^a	
	LiCl		
	Cluster	Bulk LDA	Expt.
Band gap (eV)	5.4	5.8 ^c	9.2
Atomic spacing (a.u.)	4.91		4.86
Bulk modulus (Mbar)	0.36		0.30
F -center level (eV)			

^aReference 13.

^bReference 12.

^cReference 14.

between the central O atom and the first Mg shell.

The cluster estimate of the bulk modulus is taken from the breathing-mode relaxation of the cluster with all near-neighbor spacings constrained to be the same, and evaluated at the breathing-mode minimum of 3.78 a.u. The equation used for calculating the cluster bulk modulus was derived by relating the crystal volume to that of an anion-cation pair, expressed in terms of the near-neighbor separation. Explicitly,

$$B = -(1/18Na)d^2E/da^2$$

where N is the number of anion-cation pairs in the cluster (13.5), and a is the near-neighbor separation at the breathing-mode minimum. The curvature of the E versus a curve is taken from a polynomial fit of the calculated data.

The overall agreement of the cluster-derived properties with the corresponding bulk band structure results is very good. The band gap and lattice parameter are within a few percent of the bulk values, and the bulk modulus is within about 10%. Note that the calculated values for the band gap reflect the well-known LDA underestimation of insulator and semiconductor gaps. The cluster value for the occupied F -center energy level is somewhat underestimated, i.e., the F -center states in the cluster are too close to the top of the valence band. This is perhaps due to the influence of the surface states in the gap. To first order, an interaction between these states would lower the energy of the gap states and raise that of the surface states. The cluster result for the near-neighbor distance slightly underestimates the bulk values, indicating overbinding in the cluster as compared to the bulk. This result is consistent with the overestimation of the bulk modulus in the cluster calculations.

A similar comparison of the cluster-derived properties of LiCl with the bulk values is given in Table II. Again it is seen that the cluster estimates are generally in good

agreement with the corresponding bulk values. The details of the comparison are noteworthy, however, as they indicate the difference in using charged versus neutral clusters for the cluster studies. Note, for example, that the cluster band gap is smaller than the bulk LDA band gap for LiCl, whereas it was overestimated in the MgO cluster. Physically, one expects the band gap to be overestimated in cluster calculations, converging to the correct value with increasing cluster size as the valence and conduction bands are broadened with the addition of more states to the bands. However, in the negatively charged LiCl cluster, the presence of the extra valence-band electron raises the energy of the valence-band states relative to the conduction-band states, decreasing the gap. To show this, we calculated the value of the gap for a neutral cluster at the breathing-mode minimum finding 5.8 eV; the corresponding value of the gap for the negatively charged cluster for the same nuclear configuration is 5.2 eV. The bulk LDA band gap is 5.4 eV.

The extra negative charge of the LiCl cluster may also affect the cluster bonding somewhat, affecting the cluster near-neighbor distance estimate. As mentioned in an earlier section, we investigated this directly by repeating the pure-cluster calculations for LiCl using a neutral 27-atom cluster. Using the two-step relaxation scheme described in Sec. III A, we found a near-neighbor spacing of 4.88 a.u. for the neutral cluster, which is very close to the value of 4.91 a.u. found for the negatively charged cluster. We note that the extra electron in the negatively charged cluster goes into a molecular-orbital state made up exclusively of orbitals on the (111) shell of Cl atoms, i.e., on the outermost shell of atoms in the cluster. The extra electronic charge is thus spread out over the cluster exterior, reducing its effect on the bonding in the cluster interior.

D. Comparison with other calculations

While there are no direct experimental measurements of defect-induced lattice relaxation in the two systems studied here, other theoretical results have appeared in the literature. Meng and Kunz¹ have studied LiCl:Cu⁺ using a Hartree-Fock-based embedded-cluster approach, and report a calculated 5.1% outward relaxation of the near-neighbor ions. In this approach, the central ion and the six near-neighbor ions are treated directly using the unrestricted Hartree-Fock theory. The small central cluster is then embedded self-consistently in a larger cluster of ions represented by empirical shell-model potentials. Moine *et al.*,² used a less sophisticated embedded-cluster procedure based on the multiple scattering X_α formalism to calculate a 15.9% outward relaxation of the near-neighbor ions in LiCl:Cu⁺. This calculation also treats only the central atom and the six near neighbors directly. An array of point ions outside the central cluster is used to model the coupling of the cluster to the host crystal.

A reasonable upper limit to the amount of defect-induced lattice relaxation expected in LiCl:Cu⁺ is the difference in the Cu and Li free ion radii (0.96 versus 0.78 = 0.18 Å). The result of Moine *et al.*, a relaxation of

0.41 Å, exceeds this upper bound by a factor of 2, possibly as a result of the embedding procedure used. On the other hand, Meng and Kunz's estimate (0.13 Å) is compatible with the limit set by the simple comparison of radii. Some care must be taken in comparing our result of essentially no relaxation with that of Meng and Kunz. While their result is apparently much larger than ours, we note that it is obtained by comparing the relaxed near-neighbor distance in the defect cluster with the experimental host lattice spacing, rather than the near-neighbor distance obtained using the same formalism on the pure cluster. The difference may be significant in comparing the results. For example, Vail *et al.*¹⁵ studied pure clusters to check the consistency of the embedded-cluster model, and found the pure-cluster near-neighbor distance (with the cation at the origin) to underestimate the experimental separation by 3% for NaF. The corresponding pure-cluster near-neighbor separation for LiCl was not given, but if we take the NaF result to establish a typical margin of error for predictions of alkali-halide lattice parameters by the embedded-cluster procedure, then the relaxation result obtained in Ref. 2 for LiCl:Cu⁺ may be consistent with our result of no relaxation when referenced to the calculated pure-cluster spacing.

We know of no other calculated results for relaxation in LiCl:Cu⁺.

For the MgO *F* center, an inward relaxation of the Mg ions around the *F* center of 0.9% was found by Wang and Holzwarth⁴ in a LDA-based calculation using a mixed-basis pseudopotential formulation and a large, 16-atom supercell. Pandey and Vail,³ using the Hartree-Fock-based embedded-cluster methodology described above, find an inward relaxation of 1.5% and 2% for the first and second neighbors, respectively. Both results for the first shell relaxation are in good agreement with our cluster-derived result, however, we predict a slight outward relaxation of the second shell, contrary to the result of Pandey and Vail.

IV. SUMMARY

We have reported here the results of a series of first-principles, finite-cluster calculations investigating defect-induced lattice relaxation in the ionic systems LiCl:Cu⁺ and the MgO *F* center. The finite-cluster approach is based on studying the properties of clusters in their fully relaxed ground states. While only moderately sized clusters are used, estimates of bulk pure-crystal properties taken from these 27-atom clusters are in good agreement with the corresponding bulk calculations and experiment, suggesting that reasonable results for defect-induced lattice relaxation may also be obtained using these clusters. By comparing the corresponding pure and defect clusters, our calculations yield predictions of essentially zero relaxation around the Cu ion in LiCl:Cu⁺, and a 1.3% inward relaxation of the Mg ions around the *F* center in MgO. The result for LiCl:Cu⁺ is somewhat smaller than results obtained in previous studies using embedded-cluster methods,^{1,2} but is consistent with arguments given by Harrison and Lin⁹ based on a comparison of bond lengths in CuCl and LiCl. The result for the MgO *F*

center is in very good agreement with recent first-principles supercell calculations,⁴ and with embedded-cluster results.³

We have not addressed the question of cluster size convergence directly in this work. While treating a $3 \times 3 \times 3$ atom cluster using our approach can readily be done on a modern supercomputer, the analogous $5 \times 5 \times 5$ cluster, for example, is too large to be currently practical. It would be interesting to systematically treat larger clusters to directly explore size-convergence issues, and to study, for example, the interplay between local and long-range forces in establishing cluster bonding. The calculations discussed here, however, suggest the feasibility of investigating the properties of ionic solids using the free, finite-cluster approach with clusters of moderate size. As noted above, the results obtained from the study of 27-atom clusters are in reasonable agreement with experiment for pure bulk-crystal properties, and in very good agreement with previous calculations for the relaxation around the MgO *F* center. The general approach described here has no symmetry restrictions, no restrictions to atom type, and is exact in the large cluster size limit. The same conceptual approach can be used, in principle, to treat localized, low symmetry defects of any kind.

We have not investigated charged defects in this work. (The centers treated here have the same net charge as the ions they replace in the lattice.) Because of the long-range Coulomb forces associated with charged defects, the region of the crystal affected by the defect would extend beyond the first few near-neighbor lattice shells, so that larger clusters would be required to describe these defects. It would be interesting, however, to determine how large a cluster would be required to treat charged

defects. It is possible that a reasonable description could be given using clusters that are computationally viable. Note that computer time requirements scale favorably with cluster size for our local orbital based codes. The cost of a calculation scales as N^2 , where N is the number of symmetry-independent atoms in the cluster.

We have recently altered our computer codes to include the calculation of basis set corrected atomic forces.¹⁶ We did not use the forces directly in optimizing the geometries of the clusters considered in this work, although force information was used as a check in identifying energy minima. The use of forces will substantially speed geometry optimizations. A single SCF calculation on an N -atom system yields $3N + 1$ pieces of structural information when atomic forces are calculated in addition to the total energy. This compares with the single piece of structural information provided by the total energy alone. By using forces we can treat much larger clusters than currently possible, making possible calculations on lower symmetry defects such as those on surfaces, or off-center relaxation of substitutional defects. We plan to describe applications in forthcoming publications.

ACKNOWLEDGMENTS

This work was supported in part by the U.S. Office of Naval Research. One of us (K.A.J.) acknowledges the support of the National Research Council. The calculations were carried out at the Pittsburgh Supercomputer Center, which is supported by the National Science Foundation.

¹J. Meng and A. B. Kunz, in *Atomistic Simulation of Materials*, edited by V. Vitek and D. J. Srolovitz (Plenum, New York, 1989), p. 147.

²B. Moine, H. Chermette, and C. Pedrini, *J. Chem. Phys.* **85**, 2784 (1986).

³R. Pandey and J. M. Vail, *J. Phys. Condens. Matter* **1**, 2801 (1989).

⁴Q. S. Wang and N. A. W. Holzwarth, *Phys. Rev. B* **41**, 3211 (1990).

⁵P. Hohenberg and W. Kohn, *Phys. Rev.* **136**, B864 (1964); W. Kohn and L. J. Sham, *Phys. Rev.* **140**, A1133 (1965).

⁶M. R. Pederson and K. A. Jackson, *Phys. Rev. B* **41**, 7453 (1990).

⁷S. C. Erwin, M. R. Pederson, and W. E. Pickett, *Phys. Rev. B* **41**, 10 437 (1990).

⁸J. Simonetti and D. S. McClure, *Phys. Rev. B* **16**, 3887 (1977).

⁹J. G. Harrison and C. C. Lin, *Phys. Rev. B* **23**, 3894 (1981).

¹⁰J. F. Janak, *Phys. Rev. B* **18**, 7165 (1978).

¹¹R. S. Mulliken, *J. Chem. Phys.* **23**, 1833 (1955); **23**, 1841 (1955).

¹²M. J. Mehl, R. E. Cohen, and H. Krakauer, *J. Geophys. Res.* **93**, 8009 (1988).

¹³B. M. Klein, W. E. Pickett, L. L., Boyer, and R. Zeller, *Phys. Rev. B* **35**, 5802 (1987).

¹⁴S. C. Erwin and C. C. Lin, *J. Phys. C* **21**, 4285 (1988).

¹⁵J. M. Vail, R. Pandey, and A. H. Harker, *Cryst. Lattice Defects Amorph. Mater.* **15**, 13 (1987).

¹⁶K. A. Jackson and M. R. Pederson, *Phys. Rev. B* **42**, 3276 (1990).